INVESTIGATION ON BIO-ELECTROMAGNETIC FIELD OF TERAHERTZ RADIATION BEHAVIORS AT THE INTERFACE OF BRAIN-FAT TISSUE

Muhamad Hamdi

University of Riau, Pekanbaru

Email: muh4hamdi@yahoo.com

ABSTRACT

Analysis at a boundary of brain-fat tissue has been concerned with use of terahertz radiation for fundamental studies in cellular organization and as tools in medical practice. The penetration in these two tissue is analyzed by means of numerical analysis. The 0.1-10 THz gap radiation frequency range is used for realistic theoretical analysis while it is compared to the 0.1-10 MHz and 0.1-10 GHz radiation frequency , respectively. The result of dielectric constant for brain and fat show remain constant for all frequencies in ultrasound and microwave ranges which describe dependence of dielectric constant on frequency. The sharp decrease of K in this specific THz range due to its phenomena absorbs water strongly in near infrared rotational-vibrational spectra and brain tissue included a kind of dielectric medium loss. In addition to in fact the brain tissues consist of most of glucose contained discrete tissue structures relate to water content. The result of the numerical calculation in the THz-MHz signal radiation penetration in interface of brain-fat tissue indicates reduction of electric field intensity amplitude ratio values is caused by properties of dielectric loss tissue from fat (K = 100) to brain (K = 200) and also this radiation absorbs water strongly in the liquid contained tissues. The ratio of magnetic and electric field intensity amplitude is a rise linearly with increasing ranges of higher frequencies. This fact caused besides the higher frequency the higher magnetic field intensity, also THz radiation transmission includes light emissions traveling in a straight line.

Keywords: brain-fat tissue, dielectric loss medium, interface, penetration, THz radiation

INTRODUCTION

After the introduction of the THz gap discovery in the terahertz technology as a result of the subsequent rapid development of the advanced electronics and optics method (E. Giovenale, M,2008) in this current era, it has been becoming feasible to construct medical instruments for precise analysis of the penetration, propagation and the absorption coefficient of terahertz radiation in biological medium. A notable THz ray advance technology in use for almost all research areas has been developing and improving in its innovation nowadays. Probably the next time the adaptation of THz technology will discover a radar techniques may yield the pulsed THz equipment operating in the multi-terahertz range. Since that time numerous techniques have been developing which permit utilization of terahertz in the frequency range from about 10 GHz - 10 THz (the arbitrary boundary with " phononic-photonic " transition). The extension of the effective range to 100 THz can be foreseen with the further development of Brillouin scattering techniques. In this and next analysis pursuing our individual research interest have been employing terahertz radiation method in

biologically oriented studies. It focuses on use of this radiation for fundamental studies in cellular organization and as tools in medical practice. More detail information relating to the modes of interaction of terahertz radiation energy with tissue structures is continually being sought. In biological tissue layer, penetration of terahertz radiation is the way by which the energy of a photon is taken up by biomaterial, typically the electrons of an atom in cell. Thus, the terahertz radiation energy is transformed to other forms of energy for example, to heat. Basically more complicated configurations of biological tissues and interfaces may arise in practice. However, the effects on the magnetic and electric field intensity amplitude of its penetration within a simple biological medium as choice of brain-fat tissue layer has been considered in this discussion dealing with the physical mechanisms of penetration. In this paper investigates numerically the dependence of dielectric constant on this frequency for the higher frequencies range such as the (0.1-10) THz gap range (X. C. Zhang ,2009) . Besides it analyzes the behaviors of electric and magnetic field intensity amplitude in normal for tangential and normal component, energy flux per unit area at an interface of the brain-fat tissue layer. The biological medium properties for simplicity such as tissue layer a suitable formulations can be derived. For requirement of charge cell in tissue layer assumes their characteristic of in tissue layer such as non linier, anisotropic and dielectric loss media. It is derived the boundary ('jump') conditions on the field vectors at an interface between the first and second tissue layer.

Theoretical Consideration. In analysis of the biological tissue layers electrical properties of a medium are specified by its constitutive parameters are permeability μ, permittivity ε and conductivity σ . For the simple reason the physical magnetic and electric field intensity Maxwell's equations are set in the time-domain is the most natural approach. It starts with the following main Maxwell's equations.

$$\nabla \times \mathbf{E} = -j\omega\mu\mathbf{H} \tag{1}$$

$$\nabla \times \mathbf{H} = (j\omega\varepsilon + \sigma)\mathbf{E} \tag{2}$$

$$\nabla \bullet \mathbf{H} = 0 \tag{3}$$

$$\nabla \bullet \mathbf{E} = \rho_v / \varepsilon \tag{4}$$

Fields arise from currents **J** and charges ρ_v on the source (**J** is the volume current density in A/m^2 and ρ_v is volume charge density in C/m^3). In this condition , the electric (**E**) and magnetic (**H**) field intensity, current density (**J**) are three-dimensional vector fields that are dependent on both time and space. Derivation of the wave equation for **E** with taking the curl of both sides is given Eq.(5) expression with volume charge density ρ_V as a distance function *r*.

$$\nabla^2\mathbf{E} = (-\omega^2\varepsilon\mu\sigma + j\omega\mu\sigma)\mathbf{E} \quad \text{or} \quad \nabla^2\mathbf{E} = \gamma^2\mathbf{E} \tag{5}$$

with the its general wave solution forms $\mathbf{E} = \mathcal{R}\left\{ \left| \mathbf{E}\, e^{\,j(\mathbf{kr} \pm \omega t)} \right| \right\}$ .The magnetic field vector is obtained from Maxwell's first equation

$$\mathbf{H} = \frac{\nabla \times \mathbf{E}}{-j\omega\mu} = \frac{\nabla \times \mathbf{E}_0 e^{j(\beta\mathbf{r} \pm \omega t)}\hat{\mathbf{r}}}{-j\omega\mu} \tag{6}$$

∇ in spherical coordinate , β wave propagation constant and $\mathbf{E}_o$ electric field intensity amplitude. The propagation constant γ is that square root of γ^2 whose real and imaginary parts are positive $\gamma = \alpha + j\beta$ with

$$\alpha = \omega\sqrt{\frac{\mu\varepsilon}{2}\left(\sqrt{1+(\frac{\sigma}{\omega\varepsilon})^2}-1\right)} \quad \text{and}$$

$$\beta = \omega\sqrt{\frac{\mu\varepsilon}{2}\left(\sqrt{1+(\frac{\sigma}{\omega\varepsilon})^2}+1\right)} \tag{7}$$

Attenuation coefficients are used to quantify different media according to how strongly the transmitted THz amplitude decreases as a function of frequency.

Interface Of The Two Biological Tissue Layer. Study has been concerned with THz radiation fields which can be quantitatively described in terms of a " nonlinear "analysis.

That is, it is assumed that the change in the density of the tissue layer is linearly proportional to the change in the pressure which waves are of infinitesimal radiation field intensity amplitude. Radiation pressure a can exert steady forces on interfaces between tissue layers having different values of radiation velocity and/or density. The force of radiation pressure at a plane interface is dependent on the relative amounts of incident energy reflected and transmitted or absorbed and is quantitatively equal to the difference in the energy densities in the two tissue layer. The radiation pressure P_r exerted at an interface of two tissue layers can be expressed in velocity v_1, v_2 and intensity I, that is , (M. Gantri, H. Trabelsi et al, 2010)

$$\mathbf{P_r} = (\frac{1}{v_1} - \frac{1}{v_2}) I_0 e^{j(\mathbf{k.r} \pm \omega t)} \tag{8}$$

with physical configuration as nonreflecting interface ($r_{21} = 1$), normal incidence. Maxwell equation (3) is the first boundary conditions at the interface between two tissue layers. It uses the important integral theorem or a divergence theorem . If this theorem used on the surface integral of magnetic field normal line component, then each of part of this integral is zero. Detail explanation each boundary of space is given

$$\oint_S \mathbf{B} \cdot \hat{\mathbf{n}} \, da = \oint_{S_1} \mathbf{B} \cdot \hat{\mathbf{n}}_1 \, da + \oint_{S_2} \mathbf{B} \cdot \hat{\mathbf{n}}_2 \, da + \oint_{S_3} \mathbf{B} \cdot \hat{\mathbf{n}}_3 \, da = 0 \tag{9}$$

Now in Figure 1 it lets $h \to 0$,

$$\oint_{S_1} \mathbf{B} \cdot \hat{\mathbf{n}}_1 \, da - \oint_{S_2} \mathbf{B} \cdot \hat{\mathbf{n}}_2 \, da = 0 \tag{10}$$

n's are in opposite directions. At interface of Eq.(9) is obtained the requirement : $B_{1n} = B_{2n}$. Analysis on the surface part results in the equation

$$\oint_S \nabla \times \mathbf{E} \cdot \hat{\mathbf{n}} \, da = -\oint_S \frac{\partial \mathbf{B}}{\partial t} \cdot \hat{\mathbf{n}} \, da = 0 \tag{11}$$

Eq. (11) relation to electric field intensity amplitude **E** in the closed line integral with the surface integral of magnetic field **B** in normal direction is given

$$\oint_S \mathbf{E} \cdot d\ell = -\oint_S \frac{\partial \mathbf{B}}{\partial t} \cdot \hat{\mathbf{n}} \, da \tag{12}$$

or the tangential component of electric field intensity amplitude E_t is continuous in interface. The left part of Eq (12) may be resulted in the next equation expression

$$E_{1t} - E_{2t} + h_1 E_{1n} + h_2 E_{2n} - h_1 E'_{1n} - h_2 E'_{2n} = -\oint_S \frac{\partial \mathbf{B}}{\partial t} \cdot \hat{\mathbf{n}} \, da \tag{13}$$

(a)   (b)
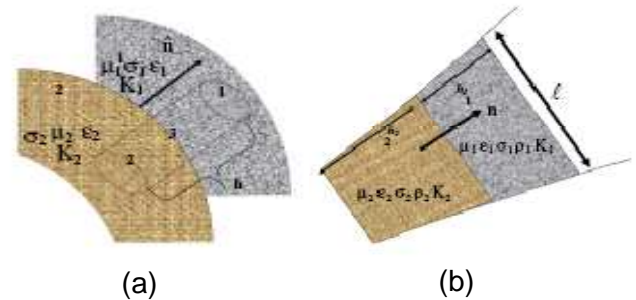
Figure 1. A small tissue layer of the space between 1 tissue with biological properties $\sigma_1, \varepsilon_1, \mu_1, K_1$ and 2 tissue with $\sigma_2, \varepsilon_2, \mu_2, K_2$, and border 3 : (a) in normal direction of a small cylinder (b) in width and depth boundary

Now shrink loop, letting h_1 and $h_2 \to 0$. So h terms vanish and so does right hand side, provided only that $\frac{\partial \mathbf{B}}{\partial t}$ is bounded so $E_{1t} - E_{2t} = 0$. For $\nabla \cdot \mathbf{D} = \rho_v$ and letting $h \to 0$, $(\mathbf{D} \cdot \hat{\mathbf{n}}_1)A + (\mathbf{D} \cdot \mathbf{n}_2)A = \sigma A$ is obtained $D_{1n} - D_{2n} = \sigma$, from conservation of charge ,

$$\int_V \nabla \cdot \mathbf{J} \, dv = -\int_V \frac{\partial \rho}{\partial t} dv \text{ is given}$$

$$\oint_S \mathbf{J} \cdot \hat{\mathbf{n}} \, da = -\frac{\partial}{\partial t} \sigma A \tag{14}$$

Now letting $h \to 0$, they are obtained some equations such as $J_{1n} - J_{2n} = -\frac{\partial \sigma}{\partial t}$, $D_{1n} - D_{2n} = \sigma$

and $J_{1n} - J_{2n} = j\omega\sigma$. If light is monochromatic and σ varies as $e^{-j\omega t}$, then Eq (15) expressed in electric field intensity **E** on interface of two tissue layer which permittivity ε connecting with dielectric constant K in $\varepsilon = K\varepsilon_o$, K for biological medium depends on frequency then Eq.(14) is given the following equation

$$E_{21} = \frac{E_{2n}}{E_{1n}} = \frac{(\sigma_1 - j\omega K_1(\omega)\varepsilon_o)}{(\sigma_2 - j\omega K_2(\omega)\varepsilon_o)} \qquad (15)$$

Where $K(\omega)$ under the influence of static field, the dielectric constant is treated as a real number. The system is assumed to get polarized instantaneously on the application of the field. When the dielectric is subjected to alternating field, the displacement cannot follow the field due to inertial effects and spatially oriented defects. The dielectric constant is then treated as a complex quantity. The variation of real and imaginary parts of the complex dielectric constant with frequency ω is given by the Debye equation (E Pickwell, B E Cole, et al 2004)

$$K(\omega) = (K_\infty + \frac{K_S - K_\infty}{1 + \omega^2\tau^2}) - j(K_S - K_\infty)(\frac{\omega\tau}{1 + \omega^2\tau^2}) \qquad (16)$$

with τ is the relaxation time, infrared range dielectric constant K_S , and dielectric constant in this region is termed 'optical' or high frequency dielectric constant K_∞ .The magnetic field from equation (2) looks back again

$$\oint_S \nabla \times \mathbf{H} \cdot \hat{\mathbf{n}}\, da = \int_S (\sigma - j\omega\varepsilon) \mathbf{E} \cdot \hat{\mathbf{n}}\, da \qquad (17)$$

$$\ell H_{1t} - \ell H_{2t} + h_1 H_{1n} + h_2 H_{2n} - h_1 H'_{1n} - h_2 H'_{2n} =$$
$$\frac{h}{2}\ell(\sigma_1 - j\omega\varepsilon_1)E_{1n} + \frac{h}{2}\ell(\sigma_2 - j\omega\varepsilon_2)E_{2n} \qquad (18)$$

These terms $\rightarrow$ 0 when loop shrink for parts from H_{1n} to H'_{2n} and rest of from the previous reason **B₂** = 0, H_{21} = 0 and dielectric constant does not depend on frequency , then Eq. (18) becomes

$$\frac{H_{1t}}{E_{1n}} = \frac{h}{2}(\sigma_1 - j\omega K_1\varepsilon_o) + \frac{h}{2}(\sigma_2 - j\omega K_2\varepsilon_o)\frac{E_{2n}}{E_{1n}} \qquad (19)$$

It calls *h/2* the skin depth . So (*h/2*) $\sigma_2 E_{2n}$ is the total current ($J_{S\perp}$) Maxwell equation which is separated by the real and imaginary parts of a complex solution. However, equation of energy density and flux per area unit are nonlinear in radiation field. Energy flux **S** in interface of two biological tissue layers has been derived with using some approximations ,i.e.,

$$S = (\frac{\sigma_1 - j\omega K_1\varepsilon_o}{\sigma_2 - j\omega K_2\varepsilon_o}) E_1{}_n{}^2 \sqrt{\frac{K_2\varepsilon_o}{K_2\mu_o}}\, \hat{n} \qquad (20)$$

Energy flux in W/m2 sec and at the higher frequencies such as THz radiation range penetrating in biological tissue layers for its depth and heat transformation depends on kinds of tissue layers. If THz radiation electric field intensity amplitude has a source from an oscillating electric dipole , $\mathbf{p} = p_o e^{-j\omega t}\mathbf{r}$ located at the origin then the radiated power unit solid angle $\mathbf{S} \cdot \hat{\mathbf{r}}\, r^2$ is given

$$\frac{\overline{dP}}{d\Omega} = \frac{\omega^2 p^2 \sin^2\theta}{\frac{3}{2}\pi^2\varepsilon_o c^3} \qquad (21)$$

Where θ is an angle between **r** and **p** , for radiation zone differentiation with respect to space everything treated as a constant except e^{jkr} terms.

The Photo acoustic Effect. The radiation absorbed by sample according to the Bouguer-Lambert-Beer Law decreases its intensity in depth x ,

$$I_x = I_o\, e^{-\beta x} \qquad (22)$$

In which I_x is the intensity of the radiation which can be measured at the depth x in the substance with optical absorption coefficient β when I_o is the incident radiation intensity at the surface. The energy absorbed by the sample , and therefore also the portion thereof

which its transformed into heat. For sinusoidally modulated light, with the modulated amplitude ranging ΔI, the incident radiation intensity with its change given

$$dI_{abs} = \beta(\tfrac{1}{2}I_O(1 + \sin\omega t)e)^{-\beta x})dx \qquad (23)$$

The time-dependent process of heat conduction in the sample is described by the thermal diffusion equation ,

$$\nabla^2 T = \frac{1}{\alpha}\nabla T - \frac{\eta}{\chi}\frac{dI_{abs}}{dx} \qquad (24)$$

Which gives the change in temperature T in a sample of temperature conductivity α and thermal conductivity χ .

RESEARCH METHOD

Design of Experiment. The process of generation and detection of photo acoustic signals is presented in this section although a detailed derivation of the theory can be omitted. The tissue sample such as muscle, fat and brain using the cow tissue to be investigated is irradiated with the microwave and ultrasound radiation, modulated by chopper, for example, at Δx at a frequency $\omega/2\pi = \upsilon$ as comparison for studying penetration of THz radiation in biological tissue. It is as shown in Figure 2, meanwhile modeling and flow chart use THz radiation in Figure 3. It is assumed that the sample is optically and thermally homogenous. In addition, it is required that incident radiation intensity and the flow of heat both be perpendicular to the surface of the sample. Upon absorption of radiation intensity the energy of excitation is transformed into heat through radiationless transitions with a fractional yield of η . This leads to local periodic heating of the sample . By means of thermal diffusion the heat spreads through the sample and reaches the surface, where it is partly transferred to the free space present in the sample chamber, as illustrated Figure 2.

Numerical Methodology-Finite Difference Time Domain Method. There are a few popular computational electromagnetic methods such as the finite element method (FEM), the method of moments (MOM), and the finite difference time domain method (FDTD). The FEM is a numerical technique for finding approximate solutions of partial differential equations and integral equations. It is usually used in the frequency domain and each solving of the equations gives the solution for one frequency. The MOM method is based on integral equations and Green's functions. MOM is usually used in the frequency domain, and it has the advantage of dealing easily with long thin wires or thin patches. The FDTD method is a numerical technique for solving Maxwell's curl equations directly in the time domain on a space grid. Since it is a time-domain method, solutions can cover a wide frequency range with a single simulation run. Among these methods, a suitable numerical technique needs to be selected to calculate the interaction of the electromagnetic field with the human model in simulations. In these cases, a large portion of the geometries is non-perfectly conducting, which makes MOM's advantages in modeling surface currents on a perfect conductor indistinct. A function F of space and time is evaluated at a discrete point in the grid and at a discrete point in time as in Figure 3.

$$F^n(i, j, k) = F(i\Delta x, j\Delta y, k\Delta z, n\Delta t) \qquad (25)$$

where x, y, z and t are the steps in the x y and z directions and the time step.

Using a centered-difference expression for the space and time derivation and ignoring the second-order accuracy in space and time increments, we get the spatial and temporal derivatives of F as E and H .

$$\frac{\partial F(ij,k)}{\partial x} = \frac{F^n(i+1/2, j, k) - F^n(i-1/2, j, k)}{\Delta x} \qquad (26)$$

$$\frac{\partial F(ij,k)}{\partial t} = \frac{F^{n+1/2}(i, j, k) - F^{n-1/2}(i, j, k)}{\Delta t} \qquad (27)$$

It could be gotten the basic FDTD updating equations for *E* and *H* in Figure 3 given

$$E_x^{n+1}(i+1/2, j, k) = (\frac{2\varepsilon - \sigma e\Delta t}{2\varepsilon + \sigma e\Delta t})E_x^n(i+1/2, j, k) + (\frac{2\Delta\Delta}{2\varepsilon + \sigma e\Delta t})$$

$$\{\frac{1}{\Delta y}[H_z^{n+1/2}(i+1/2, j+1/2, k) - H_z^{n+1/2}(i+1/2, j-1/2, k)] -$$

$$\frac{1}{\Delta z}[H_y^{n+1/2}(i+1/2, j, 1/2 + k) - H_y^{n+1/2}(i+1/2, j, k-1/2)]\}$$

$$(28)$$

The updated value of the *E* (or *H*) field component is a function of its previous value (one time step before) and the previous value (half time step before) of the surrounding *H* (or *E*) fields at half spatial steps away. Power absorbed in the loads is calculated from Equation

$$Power = \Delta x(i,j,k) \times \Delta y(i,j,k) \times \Delta z(i,j,k) \times \sum_i \sum_j \sum_k [\frac{1}{2}\sigma(i,j,k) \times$$

$$x(E_{x(i,j,k)}^2 + E_{y(i,j,k)}^2 + E_{z(i,j,k)}^2)]$$

$$(29)$$

Where $\sigma_{(i,j,k)}$ (S/m) is the conductivity of the FDTD cell at the *(i,j,k)* location; E_x, E_y and E_z (V/m) are the magnitudes of the electric field components in the *x*, *y*, and *z* directions, respectively; $\Delta x(i,j,k)$, $\Delta y(i,j,k)$ and $\Delta z(i,j,k)$ are the dimensions of each FDTD cell at location *(i,j,k)* and the summation is performed over the hole volume of the load. A schematic diagram of the process of penetration THz radiation in biological tissue in modeling uses 1-10 THz range in width and depth boundary as in Figure 4(a). In Figure 4(b) a flow diagram shows the procedure for the estimation of tissue types. The computer program consists of a number of subroutines are done in succession and the flow-chart is shown in Figure 4(b). the process involves the building up of the element, structural tissue type, refractive index, thickness, density, conductivities and the determination of response values.
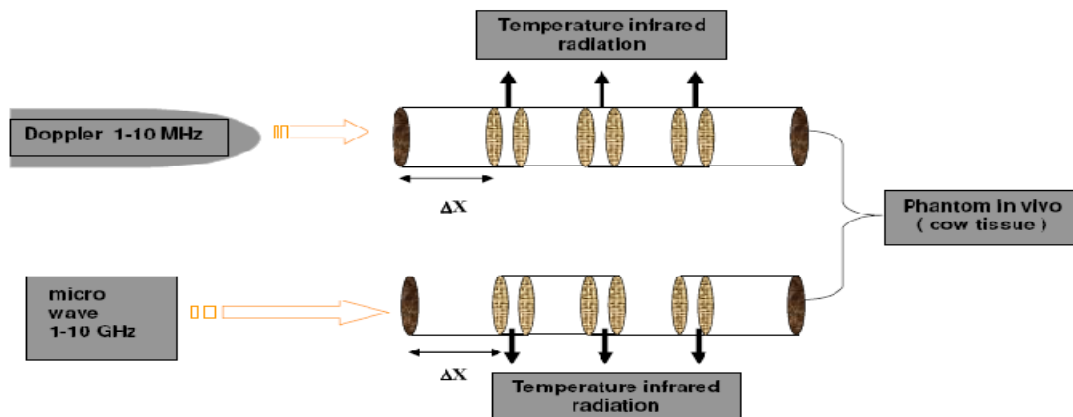
Figure 2. A schematic diagram of the process in a photo acoustic sell for cow tissue in experiment using range of frequencies in MHz and GHz
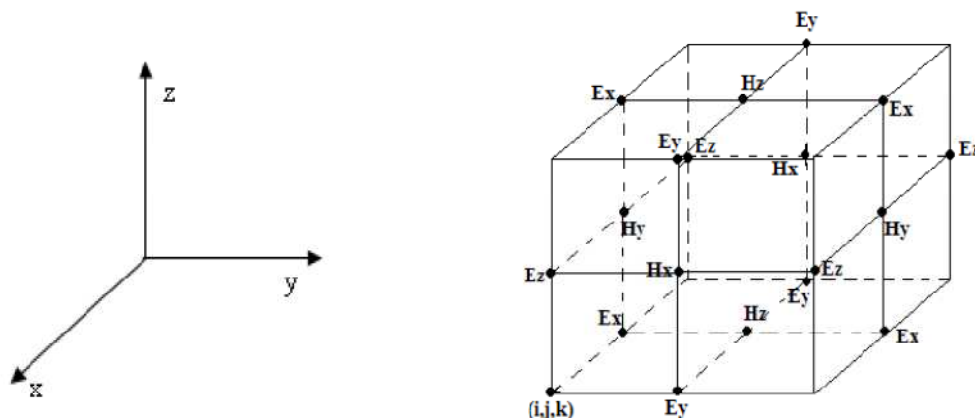
Figure 3. Yee cell shows the spatial relationship of E and H.
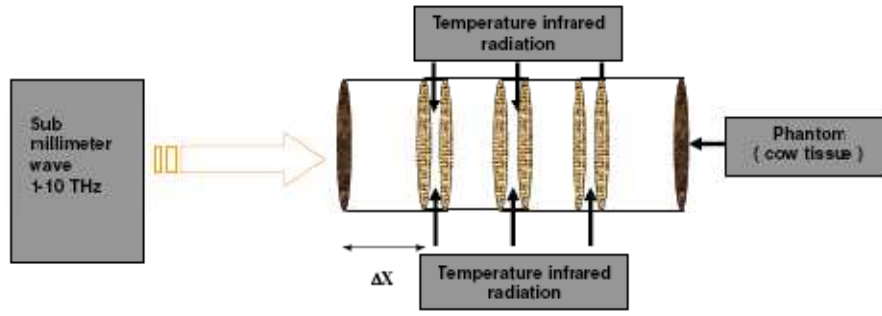
(a)
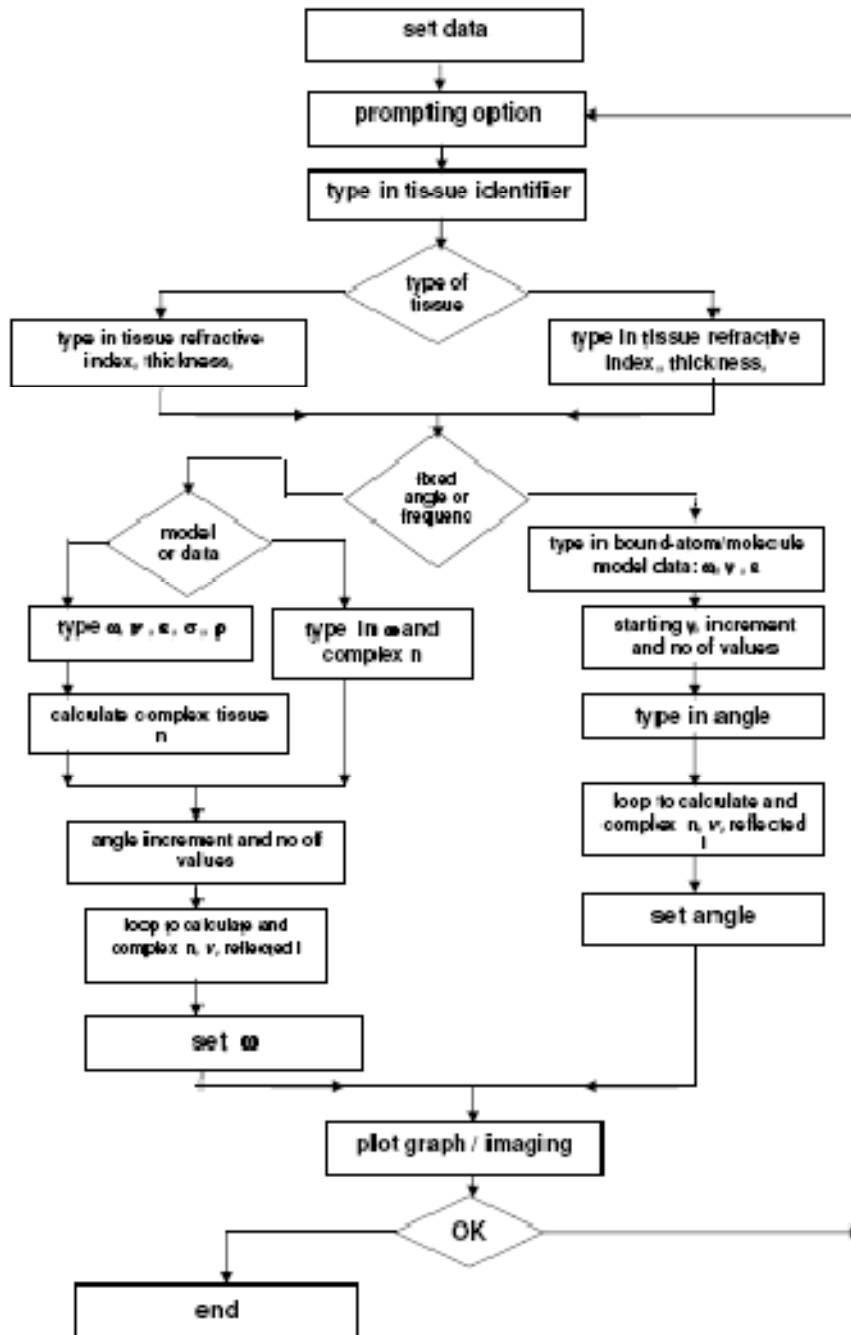
(b)

Figure 4. (a). A schematic diagram of the process in modeling using THz in width and depth boundary

(b) A brief description of program flow chart

RESULTS AND DISCUSSION

The discussions have just attempted to produce the experiment data as a comparison in MHz and GHz range to result of modeling using a numerical survey of the pertinent data on penetration of a brain-fat tissue layer boundary which may bear on the entire potential prospect of medical and biological interest. These terahertz gap ranges studied and then compared with MHz and GHz ranges for knowing the acoustic and optic properties of tissue layer as well as fluid in cell when these radiation penetrate at a boundary of brain-fat tissue layer. In biological tissues have properties of heterogeneous nonlinear and anisotropic medium, the dielectric constant K of tissue depends on frequency of radiation source. In fact, the last research result in most of references used the Debye equation (E Pickwell, B E Cole, et al 2004) had just analyzed until the high frequencies in MHz ranges, then modified use of Cole-Cole equation (M. Gantri, H. Trabelsi et al, 2010) in GHz ranges. Figure 5(a), it based on Eq.(16) has used the higher range (0.1-10 THz) in near infrared frequencies shows that dielectric constant K depending on frequency for brain and fat tissue, respectively. The result of dielectric constant for brain K = 200 and fat K = 100 show remain constant for all frequencies in ultrasound and microwave ranges which describe the independence of dielectric on frequency. The change of K occurred when this penetration of radiation in brain tissue specific for frequencies of THz ranges form 0.1 THz to 30 THz indicates decrease slightly from 28.5 THz (K=190), 29.5 THz (K=150) to 29.8 THz (K=102), and then decreases sharply at 29.9 THz (K = 75) and 30 THz (K= 43). The sharp decrease of K in this specific THz range due to its phenomena absorbs water strongly in near infrared vibrational spectra and brain tissue included a kind of dielectric medium loss. In addition to in fact the brain tissues consist of most of glucose contained discrete tissue structures relate to water content. This result also shows the same condition for fat tissue (from 29 THz (K= 90.7) to 30 THz (K=21.5).

The result of the numerical calculation in the THz-MHz signal radiation penetration in interface of brain-fat tissue layer indicates that using for frequency of 1 MHz is able to result in the tangential electric field amplitude ratio 7.29 %, frequency of 1 GHz 7.27 % and frequency of 1 THz 7.24 %.The comparison of the third frequency range is used for the penetration analysis in brain-fat interface describes that from the value of its the tangential electric field amplitude ratio for radiation signal of 1 THz is the more deeper in penetration than radiation signals of 1 MHz and 1 GHz.

The changes of electric field intensity amplitude ratio values, the part of its real value in Eq.(15) given in Figure 5(b) tends decrease from the MHz to THz range. This reduction is caused by properties of dielectric loss tissue from fat (K = 100) to brain (K = 200) and also this radiation absorbs water strongly in the liquid contained tissues. This fact probably as an indication shows the good potential clinical prospect for appropriate THz frequencies range in the future medical application. Line-of-sight propagation in a boundary of brain-fat tissue layer refers to THz electro-magnetic radiation or MHz and GHz range acoustic wave propagation in Figure 5(c).This graph describes the ratio of magnetic and electric field intensity amplitude a rise linearly wit increasing ranges of the higher frequencies. This fact caused besides the higher frequency the higher magnetic field intensity, also THz radiation transmission includes light emissions traveling in a straight line. Figure 5(d) the terahertz radiation penetrating at the boundary of brain-fat tissue layer can reduce its electric field intensity amplitude which consequences, of course, decrease its energy flux. This reduction factor is many causes of its loss ; the losses actually may have a source from diffraction, refraction, scattering, transmission or absorption. Frequencies between approximately 0.1 and 30 THz, can penetrate through brain-fat tissue layer, thus giving THz radiation transmissions in this range a potentially global reach, again along multiply

diffracted curve lines in ratio of electric field intensity amplitude and energy flux quadrate for distribution of energy flux per unit area as a complex function as can be seen in Figure 5(e). The effects of multiple diffraction lead to macroscopically "quasi-curved paths". The complex equation of real part in energy flux rate **S** for the THz (0.1-10) radiation range is described in gradient contour for flow in normal direction in area of S_x and S_y component , respectively. It show that image of flux lines change as quadrate of electric field intensity amplitude at boundary of brain-fat tissue layer. One future area of research in which penetration figures strongly is really probable in THz physics. Accounting for penetration effects in terahertz radiation is important because a reduced electric field intensity amplitude can affect the quality of the image produced. By knowing the penetration that an terahertz radiation experiences traveling through a tissue medium, one can adjust the input signal amplitude to compensate for any loss of energy at the desired imaging depth.

(a)

(b)

(c)

(d)

(e)
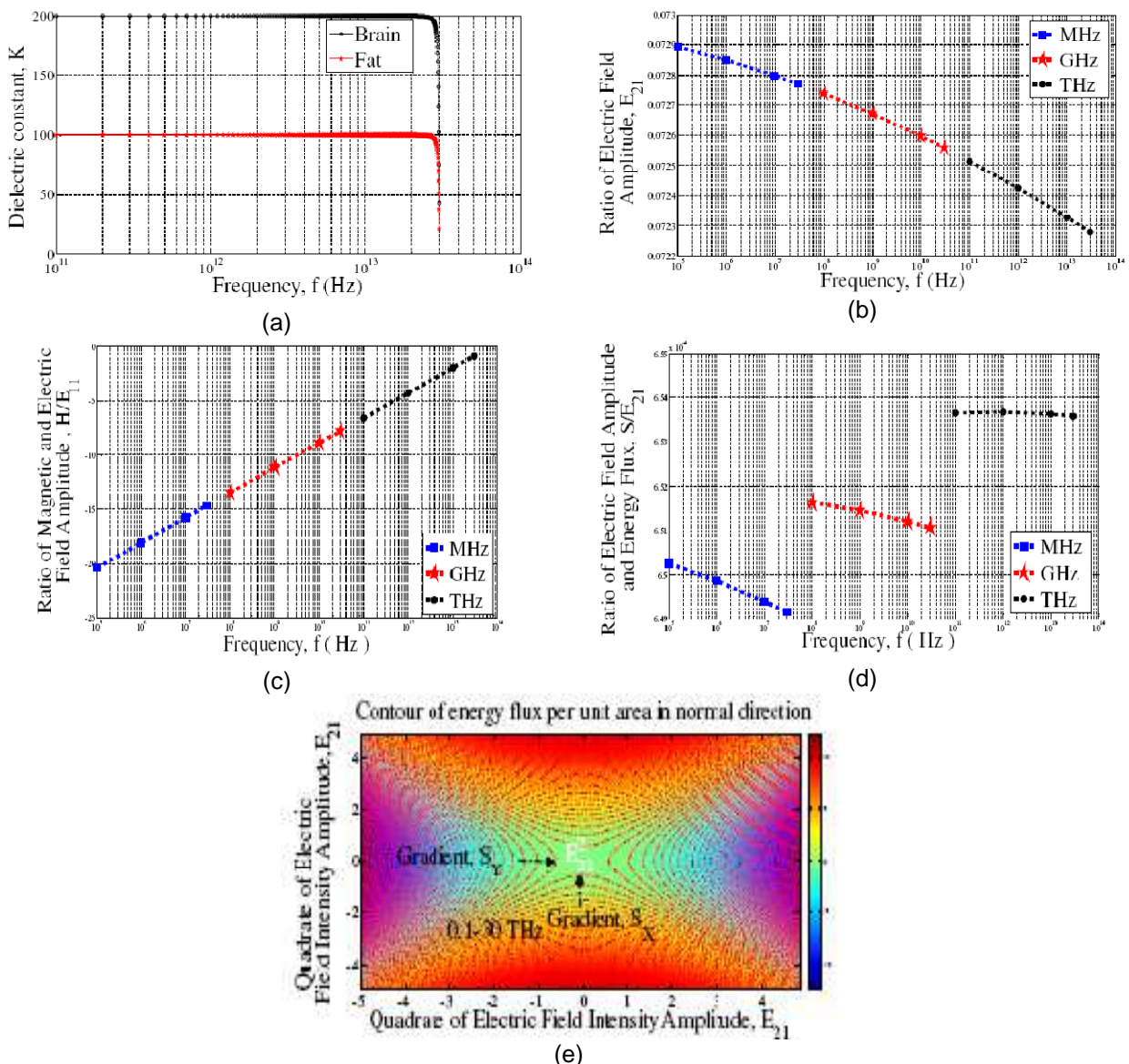
Figure 5. Numerical analysis in (a) Dielectric constant as frequency function in THz range for muscle and brain tissue, (b) The tangential electric field amplitude and (c) magnetic and electric field amplitude as well as (d) electric field amplitude and energy flux ratio of the radiation penetration in interface from the muscle (1) to brain (2) layer for MHz (ultrasound) ,GHz (phononic- photonic transition) and THz (photonic) frequencies range, (d) THz radiated power per unit solid angle in frequency range. (e) Contour of gradient of energy flux per unit area at interface of brain-muscle tissue in normal direction.

CONCLUSION

The investigation of numerical analysis emphases behaviors of terahertz radiation at a boundary of brain-fat tissue layer as an example, uses the higher range (0.1-10 THz) in near infrared frequencies shows that dielectric constant K depending on frequency for brain and fat tissue, respectively. The 0.1-10 THz gap [1] radiation frequency range is used for realistic theoretical analysis while it is compared to the 0.1-10 MHz and 0.1-10 GHz radiation frequency range. The discussions have just attempted to produce a numerical survey of the pertinent data on penetration of a brain-fat tissue layer boundary which may bear on the early potential prospect of medical and biological interest. The derivation of the new formulas follow the terahertz radiation properties relate to approaches of the biological medium physical characters and properties. They are important for example in calculating at least approximately for the dielectric constant dependence on frequency in dielectric medium with loss using these high frequency ranges. The changes of the terahertz radiation magnetic and electric field intensity amplitude and energy flux penetrates at an interface with non reflecting and normal incidence. The penetration in these two tissue layer is analyzed by means of numerical analysis. The energy flux rate in complex function as a function of electric field intensity amplitude quadrate penetrates at an interface of a brain-fat tissue layer. Since any biological tissue layer mainly consist of water, it behaves as a dielectric with losses. Dielectric constant of brain and fat tissue also show that in these specific radiation frequencies they are highly depending on the frequency. Information of the formulas are also useful in the design of THz instruments and in fact probably as an indication shows the good potential clinical prospect, where considerations of energy transfer from transducer to the biological tissue of interest arise. The most useful interaction information of terahertz radiation with tissue occurs due to strong absorption and scattering. This is in fact that if it really absorbs water in any tissue layer which it penetrates with the motion of groups of relatively large groups of molecules; in consequence, such applications sensing to medicine and biology.

ACKNOWLEDGMENT

REFERENCES

Arnold D. Kim, 2009. Transport Theory for Light Propagation in Biological Tissue, J. Opt. Soc. Am. A/Vol. 21, No. 5.

E. Giovenale, M. D'arienzo, A. Doria, G.P. Gallerano, A. Lai, G. Messina And D. Piccinelli. 2003 , Absorption and Diffusion Measurements of Biological Samples using a THz Free Electron Laser. Journal of Biological Physics 29: 159–170, Kluwer Academic Publishers. Printed in the Netherlands.

E Pickwell, B E Cole, A J Fitzgerald, M Pepper and V PWallace, 2004. In Vivo Study of Human Skin Using Pulsed Terahertz Radiation, Institute Of Physics Publishing Physics In Medicine And Biology ,Phys. Med. Biol. 49 1595–1607 Pii: S0031-9155(04)75163-5.

M. Gantri, H. Trabelsi, E. Sediki, and R. Ben Salah. 2010 ,Computational Laser Spectroscopy in a Biological Tissue, Hindawi Publishing Corporation Journal of Biophysics Volume, Article ID 253763, 9 pages doi:10.1155/2010/253763.

S. Zhang, W. Fan, N. C. Panoiu, K. J. Malloy, R. M. Osgood, and S. R. J. Brueck, 2008. "Experimental demonstration of near-infrared negative-index metamaterials," Phys. Rev. Lett. 95, 137404, .

X. C. Zhang, B. B. Hu, J. T. Darrow, and D. H. Auston, 2009.THz Spectroscopy . Appl. Phys. Lett. 56, 1011 .

Xiaoji Zhou, Xia Xu, Xuzong Chen, and Jingbiao Chen, 2009. MagicWavelengths for Terahertz Clock Transitions, School of Electronics Engineering & Computer Science, Peking University, Beijing 100871, P. R. China.